Effect of Charged Residue Substitutions on the Thermodynamics of Signal Peptide-Lipid Interactions for the *Escherichia coli* LamB Signal Sequence

Jeffrey D. Jones and Lila M. Gierasch
Department of Pharmacology, University of Texas Southwestern Medical Center at Dallas, Dallas, Texas 75235-9041 USA

ABSTRACT We have used tryptophan fluorescence spectroscopy to characterize the binding affinities of an *Escherichia coli* LamB signal peptide family for lipid vesicles. These peptides harbor charged residue substitutions in the hydrophobic core region. Titrations of peptides with vesicles composed of 1-palmitoyl-2-oleoyl-*sn*-glycero-3-phosphoethanolamine and 1-palmitoyl-2-oleoyl-*sn*-3-phosphoglycerol (65:35 mol%), in conjunction with evaluation of peptide dissociation rates from these vesicles, were used to determine binding parameters quantitatively. We find that under low ionic strength conditions, point mutations introducing negatively charged aspartate residues substantially reduce peptide affinity relative to the wild-type peptide. However, the difference between wild-type and mutant peptide affinities was much lower under approximately physiological ionic strength. In addition, the lipid affinities of model surface-binding and transmembrane peptides were determined. These comparative studies with signal and model peptides permitted semi-quantitative deconvolution of signal peptide binding into electrostatic and hydrophobic components. We find that both interactions contribute significantly to binding, although the theoretically available hydrophobic free energy is largely offset by unfavorable polar-group effects. The implications of these results for understanding the potential roles of the signal sequence in protein translocation are discussed.

INTRODUCTION

In previous studies, we have demonstrated that export-competent signal sequences share the ability to interact productively with phospholipid model membranes and to adopt high proportions of α-helix in membrane mimetic environments (Briggs et al., 1985; McKnight et al., 1989, 1991; Hoyt and Gierasch, 1991a, b; Rizo et al., 1993). More recently, we have characterized the secondary structural tendencies and membrane-interactive properties of a family of peptides derived from the signal sequence of the *E. coli* LamB protein that harbor point mutations introducing charged aspartate (Asp) or arginine (Arg) residues in the hydrophobic core region (companion paper). Stader et al. (1986) found that in vivo export activity of strains harboring these point mutations depended significantly on both the nature and position of the charged residue point mutation (discussed in more detail in the companion paper).

Our biophysical characterization demonstrated that the corresponding peptides are able to insert into the bilayer acyl chain region. However, the average depth of penetration of the point charge mutant peptides (as probed by tryptophan (Trp) fluorescence) was reduced relative to the wild-type peptide. This reduction of membrane insertion potential represents a likely explanation for the reduced in vivo export activity. Also, the spectral properties of Trp residues in vesicle-bound peptides suggested that the WT and point mutant peptides enhance bilayer hydration, with this effect being most pronounced for peptides with an Asp residue in the core region. Results from this study, along with the well established coil-helix transition upon signal peptide binding to vesicles (see Jones et al. (1990) for review), indicate that the energetics of signal peptide-phospholipid interactions are likely determined by a complex function of many parameters. These include peptide secondary structural propensity as well as hydrophobic, electrostatic, hydrogen bonding, and lipid perturbation contributions to binding. A strong degree of interrelation among these parameters is almost certainly present, because of the changes that occur in both peptide and bilayer structure when the signal peptide-lipid complex is formed.

Studies from this laboratory on the LamB and OmpA systems (cited above), as well as those on the PhoE signal peptide by de Kruijff and co-workers (Batenburg et al. 1988a, b; Killian et al., 1990; Keller et al., 1992) have led to a considerable advancement in understanding biophysical properties of signal peptide-lipid complexes. However, little is known regarding quantitation of the specific forces that mediate signal peptide-lipid interaction. This information is essential to understand the nature of in vivo signal sequence interactions with membrane lipid. Furthermore, understanding the physical basis for postulated signal sequence interactions with integral protein factors is dependent on a quantitative description of signal peptide-lipid interactions, because bulk lipid is in effect the reference phase for these interactions.

Received for publication 14 February 1994 and in final form 11 July 1994.

Address reprint requests to Dr. Lila M. Gierasch, Department of Chemistry, University of Massachusetts, Amherst, MA 01003-4510. Tel.: 413-545-2318; Fax: 413-545-4490; E-mail: gierasch@chem.umass.edu.

Abbreviations used: t-Boc, tert-Butyloxycarbonyl; 5- or 12-doxylPC, 1-palmitoyl-2-(5- or 12-doxyl)stearoyl-*sn*-glycero-3-phosphocholine; Fmoc, 9-fluorenylmethoxycarbonyl; LUV, large unilamellar vesicle; N-NBD-PE, *N*-(7-nitro-2,1,3-benzoxadiazol-4-yl)diplamitoyl-*sn*-glycero-3-phosphoethanolamine; POPC, 1-palmitoyl-2-oleoyl-*sn*-glycero-3-phosphocholine; POPE, 1-palmitoyl-2-oleoyl-*sn*-glycero-3-phosphoethanolamine; POPG, 1-palmitoyl-2-oleoyl-*sn*-glycero-3-phosphoglycerol; N-Rh-PE, *N*-(lissamine Rhodamine B sulfonyl)dipalmitoyl-*sn*-glycero-3-phosphoethanolamine; TLC, thin layer chromatography.

0006-3495/94/10/1546/16 $2.00

In the present study, we have carried out a detailed characterization of peptide binding affinities of the LamB point charge mutant peptide family for model bilayer vesicles whose composition mimics that of the *E. coli* plasma membrane. This peptide family consists of sequences with Asp and Arg mutations at different positions in the hydrophobic core, as well as an Asp substitution near the C-terminus. These peptides, therefore, represent a rich system for analysis of electrostatic effects on binding. Also, this system permits comparison of binding affinities among the WT peptide and mutants with reduced ability to insert into the lipid acyl chain region (see companion paper). Because signal peptide binding is likely to depend on the several energetic terms discussed above, it is very difficult to distinguish the relative magnitudes of these terms. Thus, we also analyzed the affinity for the model surface-bound and transmembrane peptides introduced in the companion paper (see Results). Determination of the binding energy for the surface-bound peptide permits estimation of the electrostatic component of signal peptide binding. Comparison of signal sequence and transmembrane peptide binding affinities yields approximate values for the fraction of available hydrophobic energy consumed upon signal peptide association with vesicles.

Binding affinities were analyzed by titration of Trp-labeled peptides with lipid vesicles. In addition, approximate binding affinities were inferred via determination of peptide dissociation rates from vesicles using fluorescence methods. We find that both electrostatic and hydrophobic interactions contribute significantly to binding. However, the results suggest that a significant fraction of the available hydrophobic binding energy is offset by energy losses, presumably to unfavorable polar group interactions and to configurational entropy inherent in restricting the peptides to a helical conformation (Jacobs and White, 1989; see Discussion). As suggested by Dill (1990) and Sharp et al. (1991a, b), a significant correction factor derived from Flory-Huggins polymer theory (Flory, 1941; Huggins, 1941) was necessary to assess the hydrophobic binding component. Relative lipid affinities were highly dependent on ionic strength, consistent with substantial electrostatic binding energy. At near physiological conditions, binding constants were found to be in the micromolar to millimolar range. A detailed binding model is described in which signal peptide partitioning is analyzed as arising from a combination of electrostatic, hydrophobic, hydrogen bonding and lipid perturbation effects. These results are examined in the light of previous results with other membrane-interactive peptides, and the implications for understanding the potential roles of signal sequences in mediating protein export are discussed.

MATERIALS AND METHODS

Materials

All phospholipids were purchased from Avanti Polar Lipids (Birmingham, AL). Lipid purity was routinely checked by thin layer chromatography (TLC1) in $CHCl_3$/MeOH/H_2O and visualized with primulin spray.

Sample preparation

Peptides were synthesized via standard methodology using either N-terminal, t-Boc-protected amino acids (Erickson and Merrifield, 1976; Barany and Merrifield, 1979) or N-terminal Fmoc-protected amino acids (Dryland and Sheppard, 1986). Peptides were deprotected and cleaved from the resin using either anhydrous HF (t-Boc) or TFA (Fmoc) and purified on Vydac C_4 and/or phenyl columns eluted with acetonitrile/water gradients containing 0.1% TFA. Experiments were carried out using large unilamellar vesicles (LUVs) prepared via freeze-thaw extrusion (Mayer et al., 1986). Vesicle composition was 65:35 mol% POPE/POPG unless otherwise noted. Lipid concentrations were determined using an inorganic phosphate assay (Bartlett, 1959). All peptides were prepared as stock solutions in pH 3.5 H_2O and added to lipid solutions.

Peptide-vesicle titrations

All fluorescence measurements were performed on a steady-state, photon-counting spectrofluorimeter (Model Greg PC from ISS Inc., Champaign, IL) operating in the ratio mode. Trp emission spectra (excitation 280 nm) were recorded at 25°C in a 1 cm quartz cuvette. The solution was continuously stirred during measurements. For titrations carried out at low ionic strength (see Results for exact conditions), data were collected initially at the highest lipid concentration evaluated. Subsequent samples were prepared by serial dilution with replenishing of peptide and buffer to maintain constant peptide concentration. For experiments carried out under high salt conditions, each sample at a given concentration was prepared fresh, because of decreased vesicle stability at higher salt (see Results). Correction was made for excitation light scattering by subtracting background vesicle spectra. Where necessary, correction was made for emission scattering effects by analysis of pure Trp spectra.

Peptide fractional binding to vesicles

Binding of Trp-labeled peptides to vesicles results in an increased quantum yield and blue-shift of the Trp spectrum (see companion paper). These spectral changes can thus be used to quantitate peptide binding. Data were analyzed with the assumption that spectra are representative of a two-state model (bound and free peptide). Under this assumption, the fraction of peptide bound at a given lipid concentration can be calculated from intensity ratios at wavelengths that reflect bound and free peptide, given that the net intensity at these wavelengths is a sum of intensities from the bound and free states. The intensity ratio (I_r) is equal to I_l/I_h, where I_l and I_h are the intensities at the low (increases with peptide binding) and high wavelengths, respectively. The relevant equation for calculating fractional binding (F) is

$$I_r = \frac{[FI_{Bl} + (1 - F)I_{Ul}]}{[FI_{Bh} + (1 - F)I_{Uh}]}, \quad (1)$$

where $I_{B(l \text{ and } h)}$ are the intensities for bound peptide at the low and high wavelengths and $I_{U(l \text{ and } h)}$ are the respective intensities for unbound peptide. These values are determined from spectra of the bound (high lipid) and unbound peptide (no lipid). Solving Eq. 1 for F yields

$$F = \frac{[IU_l - I_r IU_h]}{[I_r IB_h - I_r IU_h - (IB_l - IU_l)]}. \quad (2)$$

Thus, the observed intensity ratio is used to calculate fractional binding in conjunction with spectra of bound and free peptide. This ratio is insensitive to absolute intensities and, thus, small changes in peptide concentration over the course of a titration, as well as inner filter effects do not affect results (bound and free intensities change proportionally). Specific examples are given in the results section.

Peptide transfer experiments

Peptide dissociation rates from POPE/POPG (65:35 mol%) vesicles were monitored according to the following procedure. Peptides were added initially to POPE/POPG donor vesicles with subsequent addition of acceptor

vesicles, which contained a quencher of fluorescence and were comprised of POPE/POPG 45:35 mol% with 20% of either 1-palmitoyl-2-(5- or 12-doxyl)stearoyl-*sn*-glycero-3-phosphocholine (5- or 12-doxyl PC). The transfer rate was monitored by measuring the time course of the decrease in fluorescence intensity upon transfer of the Trp-labeled peptides from donor to quencher-containing acceptor vesicles. The fluorescence intensities of the Trp-labeled peptides after addition either to the donor/acceptor mix or to donor vesicles of an equal concentration as the donor/acceptor mix were monitored to establish the minimum and maximum intensities, respectively.

Vesicle fusion assay

Signal peptide-induced fusion of vesicles was determined using a fluorescence assay based on the procedure described by Nichols and Pagano (1982). Fusion is monitored by following the dilution in the local concentration of lipid-labeled probes as the probe-containing vesicles fuse with unlabeled vesicles. Briefly, vesicles were prepared containing 1 mol% N-NBD-PE and 1 mol% N-Rhod-PE (63% POPE, 35% PG, 1% N-NBD-PE, 1% N-Rhod-PE). The NBD and Rhod groups are an efficient donor-acceptor pair for resonance energy transfer. These vesicles were mixed with a 10-fold excess of unlabeled vesicles (65:35% POPE/POPG) in the presence of signal peptide (G17R, see Results). Vesicle fusion is evidenced by the decrease in the 590 nm (Rhod emission maximum)/525 nm (NBD emission maximum) intensity ratio as the labeled vesicles fuse with unlabeled vesicles.

Binding model

The analysis of peptide binding to vesicles was carried out with the goal of defining a molecular partition coefficient of the peptide between the aqueous phase and POPE/POPG vesicles. Binding data were analyzed initially to yield a dissociation constant in terms of total lipid concentration. Our model for binding assumes that the interaction of peptides with vesicles arises from both electrostatic and net hydrophobic effects. Electrostatic interaction comprises both nonspecific enhanced peptide solubility in Gouy-Chapman double layers and specific binding of basic residues to PG molecules (McLaughlin, 1989; Kim et al., 1991). The electrostatic interaction component is treated as saturable in that binding of the basic residues to acidic lipids prevents these lipids from interacting with other peptides. Thus, derivation of a molecular partition coefficient must consider the specific binding component (Jain et al., 1985). Hydrophobic interaction is treated as a nonspecific partitioning process that can involve both PE and PG molecules. An equilibrium constant in terms of lipid concentration can be derived according to the general relationship

$$[PL] \rightleftarrows [P_F] + [L_F] \tag{3}$$

Therefore,

$$K_D = \frac{[P_F][L_F]}{[PL]} \tag{4}$$

where $[P_F]$ = free peptide concentration, $[PL]$ = concentration of peptide/lipid complex, and $[L_F]$ = concentration of free lipid. We wish to express K_D in terms of the known quantities $[P]$ and $[L]$, which are total peptide and lipid concentrations, respectively; and the experimentally determined peptide fractional binding to lipid, F. With the relationships $[L_F] = [L] - [PL]$ and $[P_F] = [P] - [PL]$:

$$K_D = \frac{[P] - [PL]}{([L] - [PL])/[PL]}. \tag{5}$$

Thus, with $F = [PL]/[P]$,

$$K_D = \frac{([P] - F[P])([L] - F[P])}{F[P]}. \tag{6}$$

Rearrangement yields:

$$[P]^2F^2 + [L][P] + (-[L][P] - [P]^2 - K_D[P])F = 0. \tag{7}$$

K_D values were then calculated by fitting fractional binding to lipid concentration at a given peptide concentration. This procedure permits comparison of determined K_D values at different peptide concentrations. The above treatment assumes stoichiometric binding of peptide and lipid molecules. According to our model, specific binding occurs only between basic residues and PG molecules (see below). Therefore, the fraction of specifically bound lipid per peptide depends on the mol% PG in the vesicle and the number of PG's bound per peptide. To a first approximation, it may be assumed that each basic residue binds one PG molecule and effectively removes this molecule from interaction with other peptides. Thus, binding stoichiometry is corrected by multiplying total peptide concentration by a correction factor "c", which is given by: (mole fraction PG)$^{-1}$(number of positive charges). Thus, $[P]$ is replaced by $c[P]$ and, therefore, fractional binding data are fit to

$$c^2[P]^2F^2 + [L]c[P] + (-[L]c[P] - c^2[P]^2 - K_Dc[P])F = 0 \tag{8}$$

The above procedure represents a theoretical treatment for determination of a water-lipid partition constant with correction for specific binding. We discuss below general predictions of the model and then consider their application to our experimental system. The following predictions arise from the above analysis.

1) If K_D is substantially greater than $c[P]$, the specific binding effect does not remove a significant fraction of lipid molecules from interacting with peptide. Thus, K_D is independent of $c[P]$ and binding approximates a true partitioning process.
2) If K_D is substantially less than $c[P]$, vesicle titrations yield saturable binding with a transition midpoint that varies directly with peptide concentration. Analysis of binding data under these conditions theoretically permits determination of the c value.
3) In the intermediate range where K_D is approximately equal to $c[P]$, partitioning occurs with a significant specific binding component. In this case, analysis of binding as a function of peptide concentration permits experimental determination of K_D and binding stoichiometry (Jain et al., 1985; Schwarz and Beschiavilli, 1989), which is the c term in our model.

In the system examined in the present study, specific binding arises from electrostatic interaction of peptides with vesicles. When a significant fraction of PG molecules are bound, causing surface dilution of the remaining PG molecules, both specific mass-action and nonspecifc Gouy-Chapman effects are reduced (Kim et al., 1991). As a result, electrostatic interaction decreases nonproportionally to the reduction of PG molecules. Therefore, K_D becomes a function of mol% PG, and negative cooperativity results. Therefore, assumption 3 is not adequate for treatment of this system. A more extensive treatment where binding is analyzed as a function of both PG content and of peptide concentration is necessary to derive a family of K_D values for varying PG contents. However, because of vesicle instability at high $[P]/[L]$ ratios (see Results), this was not feasible for our system. Thus, the above model is valid only under conditions where $K_D > c[P]$. Specific examples are given in Results.

It must be noted that our assumption that specific binding arises only from stoichiometric binding of basic residues to PG molecules is undoubtedly somewhat arbitrary. Nonstoichiometric binding to PG as well as specific interaction with PE headgroups may certainly occur. However, as discussed above, under conditions where $K_D > c[P]$, derived K_D values are insensitive to c and, thus, this assumption does not significantly affect the results.

The above treatment in which specific binding is considered by multiplying peptide concentration by the c factor differs from the common procedure in which lipid concentration is corrected by the "n" term, which denotes the number of lipids bound per peptide. Analysis of data using the common latter procedure according to $[P] + [nL] \rightleftarrows [PL_n]$ entails the implicit assumption of a discrete number of independent binding sites and, thus, derived affinities are dependent on the value chosen (or determined) for n. This assumption is strictly valid only under conditions where an equilibrium exists between peptides and lipid complexes of coordination number n in solution. In lipid vesicles, independent binding sites do not exist and peptide binding is more properly treated as a partitioning between two solvents (water and lipid). If specific binding of peptides to lipids exists, in

that binding of a peptide removes a given number of lipids from interaction with other peptides, the derived partition coefficient is not affected unless a significant number of lipids (about 15–20%) are specifically bound. Our analysis correctly treats specific binding, because calculated K_D values are independent of c at low $[P]/[L]$ ratios, and K_D values are corrected for specific binding at high $[P]/[L]$ ratios.

Determination of water-lipid transfer free energies

The molar partition coefficient is calculated according to

$$K_p = C_w V_w / C_l V_l, \quad (9)$$

where C is peptide concentration and V is volume; subscripts w and l denote water and lipid, respectively (Pjura, 1984). The derived K_D values yield the lipid concentration at which the peptide partitions equally between water and lipid. K_p is thus given by V_w/V_l at this lipid concentration. Peptides were assumed to partition into the outer leaflet of the bilayer vesicles (see companion paper). This represents a first approximation, because different peptides probably sample different fractions of bilayer volume. However, this method is the most straightforward for general comparison of the peptides studied. The lipid volume is assumed to be 650 cm^3/mol (Koyanova, 1990). Transfer $\Delta G°$s are typically calculated from K_p according to $\Delta G°_{tr} = RT \ln K_p$. However, recent analyses by Dill (1990) and by Sharp et al. (1991a, b), demonstrate that this expression is only valid under particular circumstances: namely, when the molar volumes of solute and solvent molecules are equivalent. Otherwise, a correction factor derived from Flory-Huggins polymer theory (Flory, 1941; Huggins, 1941) is necessary. The relevant equation is (Sharp et al., 1991b)

$$\overline{\Delta G°}_s(a \rightarrow b) = RT \ln(p^b/p^a) + RTV_s(1/V_b - 1/V_s). \quad (10)$$

For partitioning of peptides between water and lipid, this equation becomes

$$\overline{\Delta G°}_s(\text{lip} \rightarrow H_2O) = RT \ln K_p + RTV_{pep}(1/V_{H_2O} - 1/V_{lip}). \quad (11)$$

Inspection of this equation reveals that when the product of the peptide volume and the reciprocal difference in the water and lipid volumes is significant with respect to K_p (as is indeed the case), a substantial Flory-Huggins correction factor results. For simplicity of comparison among peptides, peptide volume was taken as the sum of 70% of the molar volume of each amino acid (volumes are given by Sharp et al., 1991b; proline is assumed to be 30 cm^3/mol), the volume of water is assumed to be 18 cm^3/mol (Lide, 1990).

RESULTS

Peptides studied

The peptides selected for study are shown in Table 1. Relative in vivo activities are indicated for the export-characterized signal peptides. The reduced activity of A13D relative to G17D indicates that substitution of a charged residue in the central region of the hydrophobic core inhibits export more effectively than substitution at the core periphery. Also, the fact that G17R has a significantly lower activity that G17D suggests that introduction of a positively charged residue in the core region reduces export efficiency to a greater degree than a negatively charged residue. The A13R variant has not been characterized in vivo, but was chosen for study to complement experiments examining G17R. The M24D variant was chosen as a control for a peptide with net charge equivalent to that of the core aspartate mutants, to distinguish the effect of placing a charged residue in the core and altering the general electrostatic behavior of the peptides. All signal peptides were prepared with a Trp substituted for valine at position 18 for fluorescence studies. The TM peptide was designed as an idealized transmembrane peptide. This peptide was synthesized with a Trp substitution at position 6. The KWK-AM served as a model surface-bound peptide with net charge equivalent to the N-terminal region of the signal peptides.

TABLE 1 Peptide sequences studied

		Activity
Export characterized signal peptides		
WT	MMITLRKLPLAVAVAAGVMSAQAMA	+++++
WT-AM	MMITLRKLPLAVAVAAGVMSAQAMAa	++++
G17R	MMITLRKLPLAVAVAARVMSAQAMA	++
A13D	MMITLRKLPLAVDVAAGVMSAQAMA	+
G17D	MMITLRKLPLAVAVAADVMSAQAMA	++++
Control peptides		
KWK-AM	KWKa	
A13R	MMITLRKLPLAVRVAAGVMSAQAMA	
M24D	MMITLRKLPLAVAVAAGVMSAQADA	
TM-AM	KKKKKALALALALALALALALALALa	

The signal peptides all harbor a tryptophan for valine substitution at position 18 for fluorescence studies. The TM peptide was synthesized with tryptophan at position 6 for fluorescence studies. Relative export activities are estimated based on data from Stader et al., (1986).

Peptide/lipid titrations

All peptides studied have a net positive charge near physiological pH and thus will exhibit electrostatic interaction with acidic lipid vesicles. Peptide affinities were initially evaluated at low ionic strength to compare relative affinities under conditions where maximum binding is expected. To get an initial estimate of peptide binding affinities, peptides were titrated against vesicles whose composition mimics that of the *E. coli* plasma membrane (65:35 mol% POPE/POPG). The emission maximum of the Trp residue undergoes a shift to lower wavelengths (blue-shift) upon displacement from the aqueous phase to the hydrocarbon interior (Surewicz and Epand, 1984; see companion paper for discussion of blue-shift magnitudes for this peptide family). Thus, the Trp spectral change can be used to monitor binding equilibria of the peptides to lipid vesicles. Fig. 1 shows the change in Trp emission maxima as a function of vesicle lipid concentration for the indicated peptides (see companion paper for discussion of the emission maximum in terms of mode of peptide interaction). As discussed in Materials and Methods, vesicles are titrated from high to low concentration at constant $[P]$ (low $[P]/[L]$ to high $[P]/[L]$). Thus, the Trp blue-shifts are initially at their maximum value and the decrease in blue-shift as $[L]$ is reduced is used to evaluate binding constants. For WT18W, WT-AM18W, as well as for the arginine (Arg) mutants and KWK-AM, no decrease in blue-shift is observed until peptide/lipid ratios on the order of 1/10 are reached. Within the transition region, formation of visible particulates is evident, especially for the WT and Arg mutant peptides. This change in sample appearance is evidence of significant fusion and/or aggregation as saturation of PG molecules occurs. This behavior suggests that these peptides are

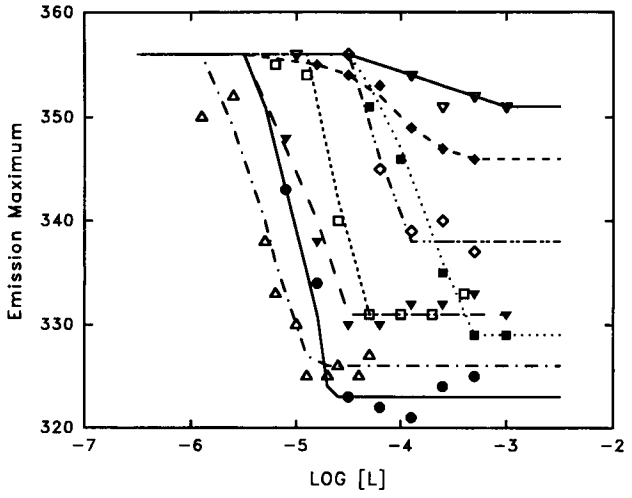

FIGURE 1 Vesicle titration of signal peptides under low ionic strength conditions. Peptide concentrations are 5 μM (A13D18W and G17D18W: 10 μM). Plots are extrapolated to solution emission maximum (356 nm in each case). Buffer composition is 5 mM Tris, pH 7.3. Curves are as follows: WT18W-AM, ●; WT18W, △; A13R18W, ▼; G17R18W, □; A13D18W, ▽; G17D18W, ♦; M24D18W, ■; KWK, ◇.

completely bound to vesicles under these ionic strength conditions, unless PG content becomes limiting. If saturation binding is indeed occurring, then the midpoint of the titration curve should vary directly with peptide concentration since binding is proportional to peptide-lipid ratio (case 2 under binding model). Fig. 2 *A* shows that this is indeed the case for KWK-AM, which indicates saturation binding. Similar qualitative results were obtained for the WT and Arg mutant peptides (not shown), although the dependence of aggregation/fusion on total lipid concentration precluded quantitative comparison. These results indicate that the WT and positively charged variant peptides, along with the KWK-AM peptide, have binding constants that are too low to measure using this procedure ($K_D \ll [P]$), because Trp fluorescence studies cannot be carried out below micromolar peptide concentrations because of the sensitivity limit of these measurements.

In contrast to the above results, titration of the Asp mutants with LUVs showed that the Trp residues on these peptides exhibit a shift in emission maximum at higher lipid concentrations than those observed for the WT and Arg-containing peptides. Fig. 2 *B* illustrates that the change in emission maximum upon vesicle titration for the core mutants is independent of peptide concentration over the range examined (a similar result was obtained for M24D18W; data not shown). Thus, for these peptides, the level of binding depends only on lipid concentration, rather than $[P]/[L]$ ratio. This result suggests that vesicle titrations with these peptides reflect equilibrium binding over this lipid concentration range. Fractional binding of the Asp mutant peptides was assessed by measuring fluorescence intensity ratios of bound and free peptide (see Materials and Methods) as a function of lipid concentration (Fig. 3). The determined K_D values (Table 2) must be viewed with caution because peptide concentration is somewhat significant with respect to lipid concentration over the range studied. This is particularly true for M24D18W (note relatively poor fit of the experimental data to Eq. 8 (Fig. 3 *C*)). Nonetheless, these data indicate that an equilibrium binding transition occurs on the micromolar concentration scale for these peptides.

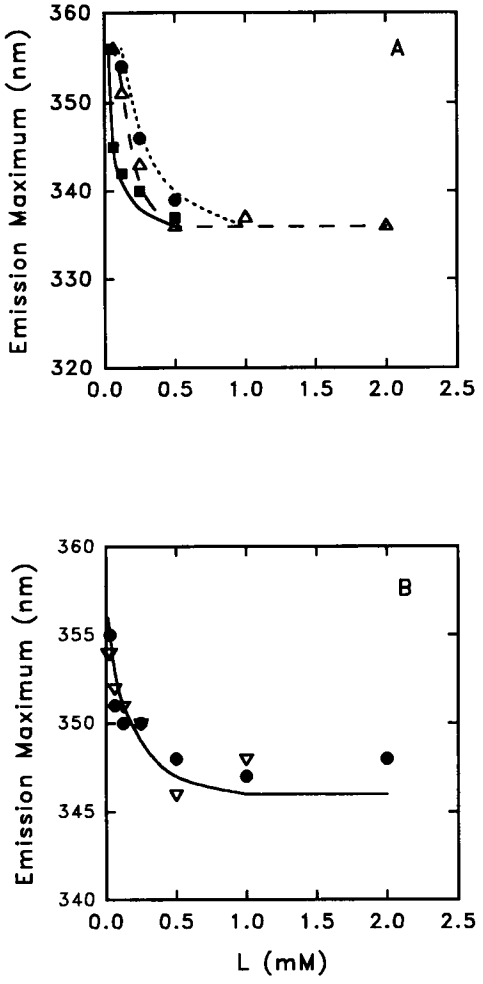

FIGURE 2 Dependence of Trp emission maximum on lipid concentration at different peptide concentration. (*A*) KWK-AM at 5 μM (■), 15 μM (△), and 20 μM (●) peptide. (*B*) G17D18W at 7.5 μM (▽) and 25 μM (●) peptide. Buffer composition is 5 mM Tris, pH 7.3.

Peptide dissociation rates

The vesicle titration results demonstrate that the affinities of the negatively charged Asp mutants for acidic PE-PG vesicles are significantly lower than those for the other signal peptides, consistent with strong electrostatic repulsion effects under these conditions. Also, the fact that similar binding constants are obtained for these mutants, regardless of the position of the Asp residue, suggests that general electrostatic effects are responsible for the reduced lipid affinity of these peptides, as opposed to a specific effect of charge placement in the core region. This conclusion is supported most strongly by the observation that the M24D18W peptide,

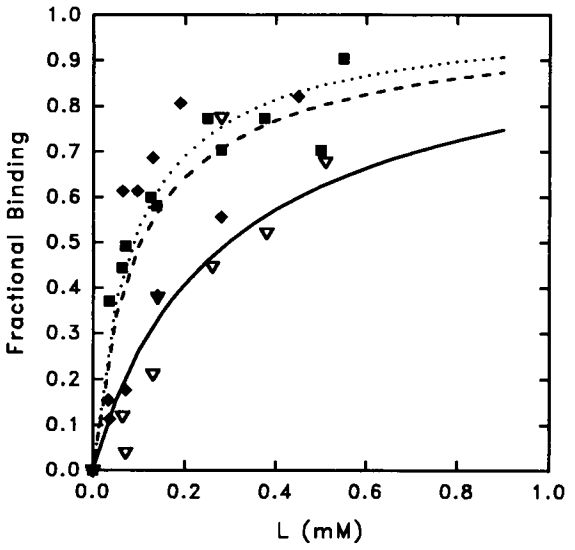

FIGURE 3 Fractional binding of Asp mutant peptides to vesicles under low ionic strength conditions. Curves are as follows: A13D18W, ▽; G17D18W, ◆; M24D18W, ■. Peptide concentrations are 15 μM for A13D18W and G17D18W and 5 μM for M24D18W. Buffer is 5 mM Tris, pH 7.3. Fractional binding is determined from intensity ratios I(335:355) for A13D18W and G17D18W and I(325:355) for M24D18W.

which has the Asp mutation near the C-terminus, binds with affinity similar to the core mutants. A quantitative comparison of lipid affinities among the Asp mutants and the WT and Arg-containing signal peptides is not possible using the vesicle titration method, because this technique only allows assignment of upper limits to binding constants for the latter peptides, because of limitations in fluorescence sensitivity. Therefore, to determine approximate binding constants for the WT and the Arg mutants, and to confirm our observation of relatively weak binding for the Asp mutants, we elected to measure peptide dissociation rates from vesicles. Measurement of peptide off-rates, in conjunction with the assumption of diffusion-controlled association rates, permits calculation of binding constants. This method has been applied previously to the study of cytochrome b_5 binding to unilamellar vesicles (Leto et al., 1980).

Rates of peptide transfer from POPE-POPG 65:35 mol% donor vesicles to acceptor vesicles containing doxyl-labeled quenchers were examined as described in Materials and Methods. Fig. 4 shows off-rate curves for: WT-AM18W (*A*), WT18W (*B*), G17R18W (*C*), M24D18W (*D*), KWK-AM (*E*), and TM-AM6W (*F*). M24D18W moves more rapidly than can be measured using this procedure, consistent with a binding constant in the micromolar range with a diffusion (or near diffusion) controlled on-rate. This result was also obtained for core Asp mutants (not shown). Likewise, KWK-AM moves too rapidly to monitor, although this peptide showed saturation binding behavior in titration experiments. Thus, the off-rate and titration studies allow assignment of approximate lower and upper limits on the K_D for KWK-AM, respectively (Table 3).

The vesicle titration studies established submicromolar binding constants for the WT and Arg mutant peptides. Theoretical estimates of binding based on available hydrophobic energy along with electrostatic interaction leads to predictions of very high binding energies (see Discussion). However, the off-rate curves shown in Fig. 4 demonstrate significant movement (seconds to minutes) for the signal peptides. WT18W and G17R18W have almost completely transferred during the dead-time of the experiment (1–2 s), although observation of the latter phase of the curve allows rough estimation of $t_{1/2}$. A similar result was obtained for A13R (not shown). The WT-AM18W peptide, however, yielded a transfer rate that was slow enough to be measured, with a half-time of 147 s determined by fitting the data to a single exponential decay curve. In contrast to these results, the model transmembrane peptide, TM-AM6W, exhibited no measurable transfer over the time course of these experiments. This result indicates that the binding affinity for this peptide is substantially greater than those observed for the signal peptides, which suggests that the hydrophobic binding energy is much higher for this peptide. The presence of the additional basic residues in TM-AM6W also enhances electrostatic interaction (see Discussion).

Inspection of the off-rate curve for WT-AM18W (Fig. 4 *A*) reveals that there is an apparent small "nonexchangeable" fraction of the peptide because the intensity never reaches the determined minimum value (also apparent for WT18W and G17R18W). However, this result cannot be concluded with certainty from the present data because the difference between the minimum of the transfer curve and the determined theoretical minimum is near the experimental error. It is possible that the binding equilibrium of WT-AM18W lies slightly toward the donor vesicles which lack quencher. Light scattering problems with the LUVs precluded extensive analysis of donor-acceptor ratio dependence. Further study with the WT-AM18W peptide is necessary for a more complete description of the transfer kinetics under these conditions. However, present results clearly indicate that this peptide exhibits exponential transfer behavior with half-times on the order of several minutes. Also, no nonexchangeable fraction was evident under physiological ionic strength conditions (see below).

Off-rate studies are subject to experimental artifacts arising from transfer of marker molecules (doxyl-labeled quenchers) and/or vesicle fusion. The absence of apparent transfer for the TM6W, which serves as an effective nonexchangeable marker, indicates that the data are not complicated by quencher movement over the time course of the experiments. Also, a vesicle fusion assay was carried out according to the procedure described by Nichols and Pagano (1982; see Materials and Methods) in which dilution of NBD-PE and Rhodamine-PE is monitored in donor vesicles. The most fusogenic peptide (G17R18W, see below) was chosen for these experiments. No significant fusion was obtained under conditions used for the off-rate studies. Only when $[P]/[L]$ ratios reached the range of 1:10 was substantial fusion

TABLE 2 Peptide binding parameters for POPE/POPG (65:35%) vesicles under low ionic strength conditions

Peptide	K_D (M)*	K_P	Transfer free energy	
			Uncorrected§	Corrected for size¶
WT-AM18W	1.4×10^{-8}	3.1×10^{10}	14.3	53.3
WT18W	1.4×10^{-8}	2.2×10^{8}	11.4	50.6
A13R18W	1.4×10^{-8}	2.2×10^{8}	11.4	51.8
G17R18W	1.4×10^{-8}	2.2×10^{8}	11.4	52.2
A13D18W‡	$2.1 \pm 0.7 \times 10^{-4}$	1.5×10^{4}	5.7	45.3
G17D18W‡	$4.6 \pm 1.5 \times 10^{-5}$	6.7×10^{4}	6.6	46.6
M24D18W‡	$6.2 \pm 3.1 \times 10^{-5}$	5.0×10^{4}	6.4	44.9
KWK-AM	5.0×10^{-6}	6.2×10^{5}	7.9	15.0
	5.9×10^{-8}	5.2×10^{7}	10.5	17.6
TM-AM6W	$<1.0 \times 10^{-12}$	$>3.1 \times 10^{12}$	>17	>62

Experiments were carried out under conditions of 5 mM Tris, pH 7.3 at 25°C.

*K_D values for WT, WT-AM, 13R, and 17R represent estimates obtained from off-rate studies under the assumption of diffusion controlled association rates. Estimated half-times are 1 s for WT, 13R, and 17R (these are order of magnitude approximations). A measured half-time of 147 s was determined for WT-AM. The values given for KWK-AM represent a range defined by limits imposed by off-rate and titration studies. The relevant equation for calculation of diffusion-controlled on-rates is $k(M^{-1}\ s^{-1}) = 4\pi N(D_p + D_v)(R_p + R_v)/1000$, where N is Avagadro's number and D and R are diffusion constants and radii, respectively. 5×10^{-5} and 5×10^{-8} were chosen as a reasonable estimates for peptide and vesicle diffusion coefficients. The radius of the peptide is negligible in comparison with the vesicle radius of 45 nm. The concentration of vesicles is calculated from the total lipid concentration assuming there are 4.0×10^4 lipids per vesicle. See text for calculation of K_p. K_D values for 13*D*, 17*D*, and 24*D* are determined from vesicle titration studies.

‡ Uncertainty estimates are SEs obtained by fitting the data in Fig. 3 to Eq. 8.

§ Uncorrected transfer free energies are calculated according to: $\Delta G^\circ_{tr} = RT \ln K_p$.

¶ Residue size-corrected transfer free energies are calculated according to $\Delta G^\circ_s(\text{lip} \rightarrow H_2O) = RT \ln K_p + RTV_{pep}(V_{H_2O} - 1/V_{lip})$.

evident (not shown). Furthermore, the transfer rate of WT-AM18W was insensitive to vesicle concentration (twofold increase), which suggests that transfer occurs via a first-order desorption process. These control experiments support the conclusion that the observed transfer rates reflect peptide transfer from donor to quencher-labeled acceptor vesicles.

The binding parameters under these low ionic strength conditions (Table 2) were obtained from the vesicle titration and off-rate methods. Approximate values for the WT-AM18W, WT18W, and the Arg mutants are inferred from the off-rate studies, and values for the Asp mutants are calculated from titration experiments. The electrostatic interaction arising from the basic N-terminal region of the signal peptides can be approximated by the binding energy for the KWK-AM peptide. The fact that the signal peptides show substantially higher binding energy than does KWK-AM suggests that hydrophobic interactions contribute strongly to binding. However, as discussed above, the significantly lower lipid affinities for the Asp mutants relative to the other signal peptides indicate that electrostatic interactions also play a substantial role in determining signal peptide-lipid interactions. The fact that the binding affinity of WT18W (free carboxy terminus) is lower than that of the C-terminal amidated WT-AM18W further supports this conclusion. The Arg mutants have affinities similar to that of WT18W, which suggests that placement of an Arg residue in the signal peptide hydrophobic core does not markedly reduce the hydrophobic binding component, although enhanced electrostatic attraction can compensate for some hydrophobic energy loss. Also, in agreement with the Asp mutant results, the position of the Arg residue makes little difference to the effect of this mutation on binding affinity, based on results at positions 13 and 17. The off-rate studies provide only an upper limit of the transfer free energy for the TM6W peptide, but it is evident that this peptide binds acidic vesicles much more strongly than do the signal peptides, which is likely because of a combination of charge and hydrophobic effects. Our previous results on signal peptide binding to POPE-POPG (65:35 mol%) monolayers showed a significantly lower binding affinity of A13D relative to WT under these ionic strength conditions, whereas G17R bound with very similar affinity to WT (McKnight et al., 1989). We have since demonstrated that A13R has a monolayer affinity very similar to G17R, and A13D and G17D show very similar affinities (K. K. Ng and L. M. Gierasch, unpublished data). These results support the conclusion that the nature of the charged residue, rather than position in the sequence, is responsible for the effect of the point mutation on affinity for the POPE/POPG 65:35% model lipid system.

Effect of ionic strength on peptide-vesicle interactions

Vesicle binding studies were also evaluated under conditions of 0.1 M NaCl (5 mM Tris, pH 7.3) to determine the effect of near physiological salt concentration on peptide affinity. Because the low salt results suggest a significant role for electrostatic interactions in determining peptide affinity, we expect binding to be significantly modulated by ionic strength conditions. It is desirable, of course, to analyze signal peptide binding under approximately in vivo conditions to model physiological behavior of these sequences accurately. However, experiments were technically difficult under these conditions because vesicle instability was more evident at the higher salt concentration. A slow enhancement of Trp blue-shifts for the WT and Arg mutant peptides was observed over time upon incubation with vesicles. The rate

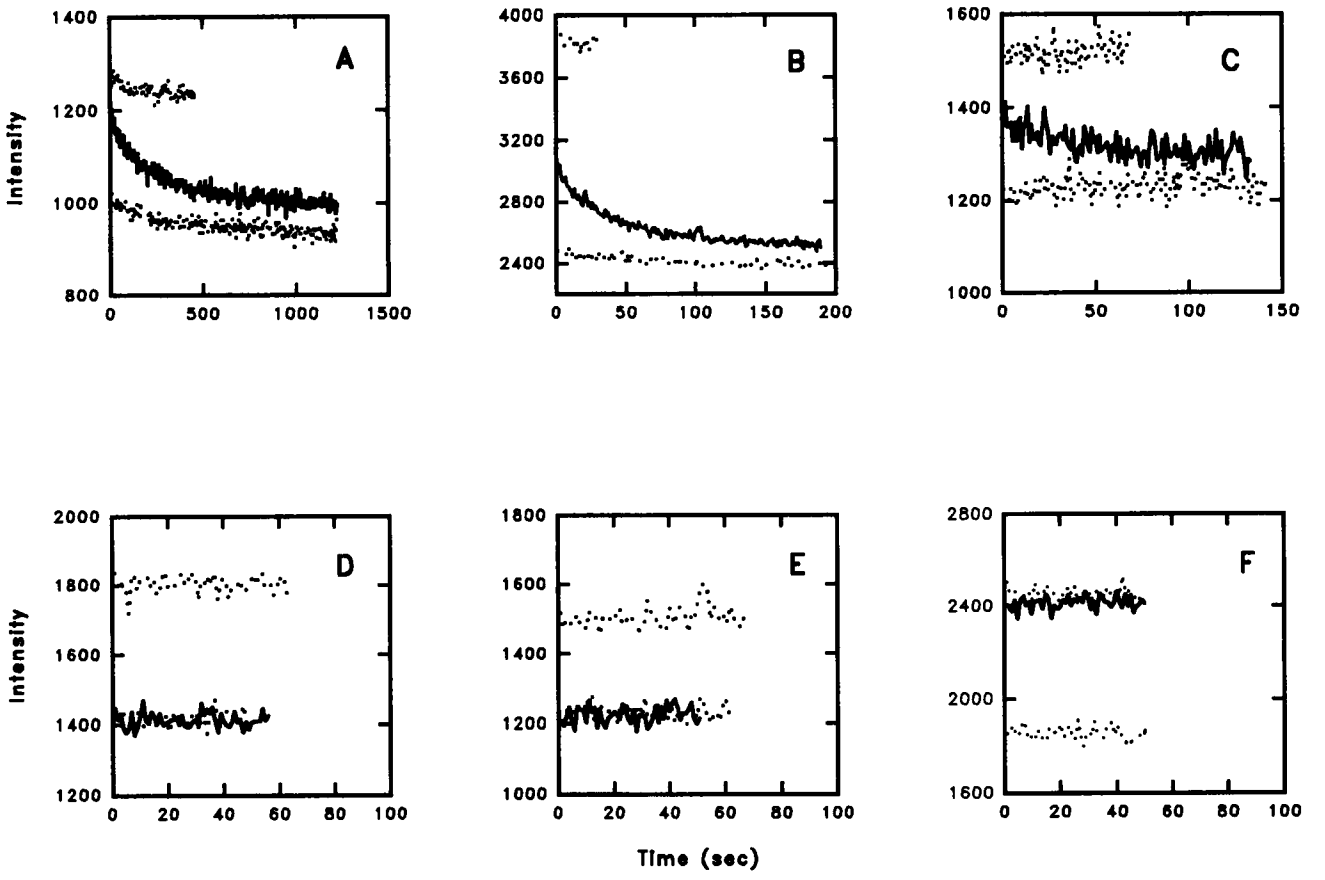

FIGURE 4 Peptide off-rates from vesicles under low ionic strength conditions. (*A*) WT-AM18W; (*B*) WT18W; (*C*) G17R18W; (*D*) M24D18W; (*E*) KWK-AM; (*F*) TM-AM6W. Peptide concentration is 5 μM, the concentration of PE-PG 65–35% donor vesicles is 0.5 mM, and the concentration of PE-PG-(5- or 12-doxylPC) 45–35–20% acceptor vesicles is 2 mM. In each case, the solid line is the peptide transfer curve, whereas the dotted lines represent maximum and minimum traces. Note that peptides are initially unquenched in donor vesicles.

TABLE 3 Peptide binding parameters for POPE/POPG (65:35%) vesicles under high ionic strength conditions

Peptide	K_D (M)*	K_P	Transfer free energy	
			Uncorrected‡	Corrected for size§
WT-AM18W	$2.3 \pm 0.7 \times 10^{-4}$	1.3×10^4	5.6	44.8
WT18W	$6.1 \pm 2.4 \times 10^{-4}$	5.0×10^3	5.1	44.3
A13R18W	$3.8 \pm 1.3 \times 10^{-4}$	8.1×10^3	5.3	45.7
G17R18W	$3.3 \pm 1.0 \times 10^{-4}$	9.3×10^3	5.4	46.2
A13D18W	1.0×10^{-3}	3.1×10^3	4.8	44.4
G17D18W	1.0×10^{-3}	3.1×10^3	4.8	44.8
M24D18W	$1.3 \pm 0.4 \times 10^{-3}$	2.4×10^3	4.6	43.1
KWK-AM	$4.1 \pm 1.9 \times 10^{-3}$	7.5×10^2	3.9	11.0
TM-AM6W	$<1.0 \times 10^{-12}$	$>3.1 \times 10^{12}$	>17	>62

Parameters were determined by vesicle titration experiments as described under Fig. 5. Conditions are 5 mM Tris, 0.1 M NaCl, pH 7.3. The spectral changes for A13D18W and G17D18W were not sufficient to determine binding constants accurately. Values given for these peptides are order of magnitude approximations.

* Uncertainty estimates are SEs obtained by fitting the data in Fig. 5 to Eq. 8 (data not shown for A13R18W).

‡ Uncorrected transfer free energies are calculated according to: $\Delta G^\circ_{tr} = RT \ln K_p$.

§ Residue size-corrected transfer free energies are calculated according to $\Delta G^\circ_s(\text{lip} \rightarrow H_2O) = RT \ln K_p + RTV_{pep}(V_{H_2O} - 1/V_{lip})$.

of this increase in blue-shift increased with increasing peptide/lipid ratio and with higher total concentration at a given peptide/lipid ratio (not shown). Thus, this change was caused by a concentration-dependent process such as vesicle aggregation or fusion as opposed to a change arising from alteration of peptide orientation in vesicles with time. The most pronounced change was for the arginine mutant peptides, presumably because their additional basic residue renders these peptides more fusogenic. Titration experiments, therefore, were carried out with each sample prepared in-

dependently, rather than by serial dilution of samples as in the low-ionic strength experiments. Data at relatively high P/L ratios were considered unreliable and were not included in the results shown in Fig. 5.

Under high ionic strength conditions, all signal peptides exhibited equilibrium binding in the concentration range amenable to peptide-vesicle titrations monitored by Trp fluorescence. Fig. 5 shows fractional binding as a function of vesicle lipid concentration for the indicated peptides. Binding data were fit using Eq. 8 as given in Materials and Methods. Comparison of titration curves at different peptide concentrations was difficult, because of the dependence of fusion/aggregation on $[P]/[L]$ ratio. However, no dependence of the derived K_D on peptide concentration was detectable within experimental error, in agreement with an equilibrium transition over this concentration range (data not shown).

The binding parameters given in Table 3 show that the WT-AM18W, WT18W, and the Arg mutants all have significantly lower lipid affinities at near physiological ionic strength than under low salt conditions, consistent with reduced electrostatic interaction caused by ionic shielding. Also, the difference in affinity between the Asp mutants and the WT and Arg mutant signal peptides is much less pronounced than it was under the low ionic strength conditions. These results suggest that, as expected, electrostatic effects are more significant under low ionic strength conditions and, thus, point mutations of negatively charged residues lead to a more marked reduction of peptide affinities at low salt. The fact that the binding constants of WT-AM18W and WT18W are within experimental error at high salt indicates that charge repulsion effects caused by the free C-terminus are likewise minimized under these conditions.

Peptide transfer studies were carried out under the higher ionic strength conditions to verify the vesicle titration results. As shown above for the Asp mutants at low salt, binding constants in the micromolar lipid concentration range translate to sub-second off-rates, if on-rates are diffusion (or near diffusion) controlled. The off-rate of the most strongly interacting signal peptide, WT-AM18W, was too rapid to monitor under these conditions, in agreement with the binding constants determined from the vesicle titration experiments (Fig. 6). Rapid net transfer, as expected, was also obtained for WT18W and the Arg mutants (not shown). By contrast, the model transbilayer peptide once again showed no movement over the measuring time of the experiment (500 s) under these conditions (Fig. 6). This result, under conditions where electrostatic attraction is minimized, strongly suggests that hydrophobic binding for this peptide is markedly greater than that for the signal peptides. Fusion assays indicated no significant fusion within the instrument dead-time at $[P]/[L]$ ratios employed in the off-rate studies.

Lipid composition dependence

Preliminary observations indicated that the WT peptide as well as the Arg mutant peptides showed saturation binding behavior at the high salt conditions when titrated against vesicles composed of 65:35% 1-palmitoyl-2-oleoyl-*sn*-glycero-3-phosphocholine (POPC)/POPG rather than 65:35% POPE/POPG (not shown). This result indicates that these peptides have significantly higher affinities for the POPC/POPG system and, therefore, affinity depends on the nature of the neutral lipid in the binary vesicles. This result may arise from lipid perturbation effects and/or bilayer hydration differences (see Discussion). However, WT18W was still observed to exhibit transfer rates that were too rapid to

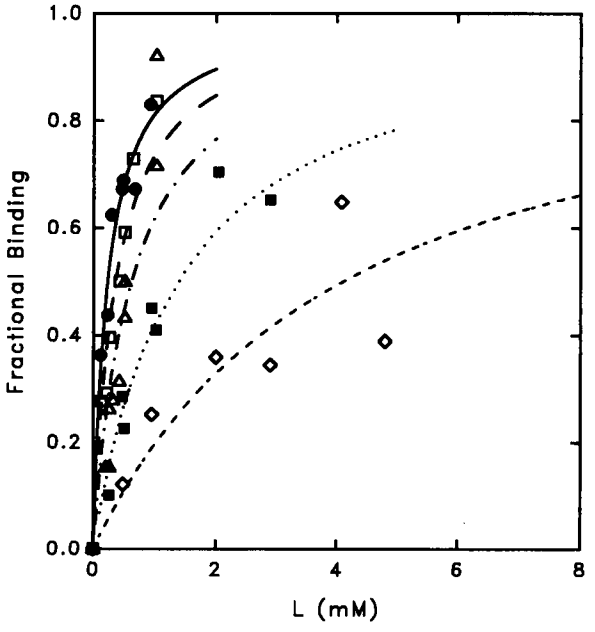

FIGURE 5 Fractional binding of peptides under high ionic strength conditions. Fractional binding was determined by computing the $I(325:355)$ ratio in each case. Curves are as follows: WT18W-AM, ●; WT18W, △; G17R18W, □; M24D18W, ■; KWK-AM, ◇. Peptide concentrations were 5 μM for WT-AM18W, WT18W, G17R18W, and KWK-AM; they were 5 or 10 μM for M24D18W. Buffer composition is 5 mM Tris, 0.1 M NaCl, pH 7.3.

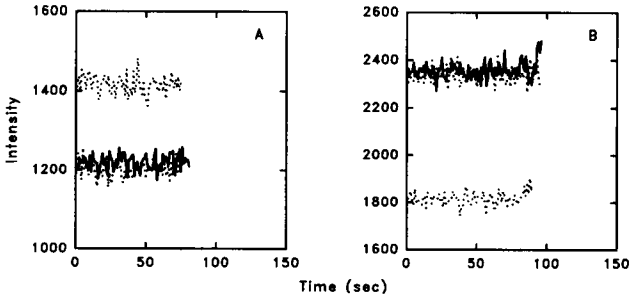

FIGURE 6 Peptide off-rates from vesicles under high ionic strength conditions. (*A*) WT-AM18W; (*B*) TM-AM6W. Peptide Concentration is 5 μM, the concentration of PE-PG 65–35% donor vesicles is 1.0 mM, and the concentration of POPE-POPG-(5-doxylPC) 45–35–20% acceptor vesicles is 2.5 mM. Buffer composition is 5 mM Tris 0.1 M NaCl, pH 7.3. In each case, the solid line is the peptide transfer curve, whereas the dotted lines represent maximum and minimum traces.

measure (not shown), suggesting that the affinity difference is not very great. Much future work is necessary to assess adequately the effect of lipid composition on interaction with these peptides.

DISCUSSION

The thermodynamics of signal peptide-lipid interactions are determined by a complex interplay of energetic factors. Our goal is to develop a quantitative description of signal peptide-lipid interactions, and to relate this description both to general features of peptide-lipid interactions and to the in vivo roles of these protein localization signals. As discussed below, a thermodynamic model based on our results and theoretical predictions shows that a substantial fraction (about 70%) of the theoretically available hydrophobic energy is lost upon signal peptide interaction with vesicles, presumably because of unfavorable polar group and lipid perturbation effects. Also, the presence of charged residues in the core region does not have a substantial effect on the hydrophobic component of signal peptide-lipid interactions.

Thermodynamic model for signal peptide-lipid interaction

Our analysis focuses on the energetics of binding for the WT signal peptide under high ionic strength conditions, which are most physiologically relevant. We will subsequently discuss the various mutant peptides and consider ionic strength effects.

After the treatment of Jacobs and White (1989), the free energy of peptide binding can be approximated using the following equation:

$$\Delta G = \Delta G(EL) + \Delta G(IM) + \Delta G(FOB) + \Delta G(POL) + \Delta G(LIP) \quad (12)$$

where *EL* denotes electrostatic effects, *IM* is the positive binding energy caused by peptide immobilization when vesicle-bound, *FOB* represents the energy gain from the hydrophobic effect, *POL* represents the energy contribution from backbone and side-chain hydrogen bonding, and *LIP* describes the lipid perturbation effect. The configurational entropy associated with formation of secondary structure is treated under the *POL* term.

Electrostatic interaction and peptide immobilization effect

The peptide immobilization effect (*IM*) is a positive entropic term that results from the loss of external degrees of freedom upon peptide binding to the bilayer. The energetics inherent in this term can be modeled as arising from a restriction of the peptide to a box that still allows some degrees of freedom. Precise estimation of immobilization energy requires a complete description of the motion of the bound peptide, which permits calculation of the net degrees of freedom lost (Jähnig, 1983; Jacobs and White, 1989). However, in the case of basic peptides binding to acidic vesicles, the entropy loss caused by immobilization is implicit in calculating electrostatic interaction energies. This term, therefore, is considered in the discussion of electrostatic binding below.

We model the electrostatic energy term as arising from the attractive electrostatic energy caused by interaction of the free N-terminus and the side chains of basic residues with the acidic PG lipids. The loss of energy arising from repulsion between free C-terminal carboxyl groups and PG molecules will be treated in the discussion on polar interactions.

The binding of polybasic peptides to negatively charged lipid vesicles has been described in detail by Kim et al. (1991). Binding can be modeled by considering electrostatic interactions as a combination of effects arising from nonspecific accumulation of peptides in the aqueous double layers surrounding the surface of charged vesicles and specific binding of basic residues to PG molecules. In the above study, data were well described by a model in which each basic residue binds to a single charged lipid headgroup. Binding energies were approximately linear with addition of basic residues. Also, binding was decreased significantly by diluting the surface charge contributed by the acidic lipids, which was successfully modeled as arising from both nonspecific interaction and specific binding; the latter was well described using mass action equations.

Our data on the KWK-AM peptide allow calculation of the net free energy from attractive electrostatic interactions of the signal peptide N-terminal region with the vesicle surface. The entropy contribution arising from the immobilization effect does not depend on peptide molecular weight and, therefore, KWK-AM is a suitable model peptide for approximating signal peptide-lipid electrostatic binding, provided appropriate Flory-Huggins corrections are made. There may be some discrepancies because of charge separation that occurs in the signal peptide, and perhaps some difference in binding between Lys and Arg residues. Also, there is some hydrophobic contribution to binding from the Trp residue. However, this contribution is negligible with respect to the potential for hydrophobic binding of the signal peptides.

Our calculated binding constant for KWK-AM at 0.1 M NaCl (4.1×10^{-3} M) is very much in agreement with those obtained by Kim et al. (1991) for binding of short polylysines to 2:1 PC/PG vesicles. The specific binding component is likely affected by the matrix lipid (POPE) and, thus, exact agreement is not to be expected. We observed a substantial ionic strength dependence, with binding energies reduced about 5 kcal/mol at 0.1 M NaCl. This effect arises from the well established shielding of electrostatic interactions by high salt (for reviews of membrane electrostatics, see McLaughlin, 1989; Honig et al., 1986). Our results with this model peptide provide a very good estimate of the attractive electrostatic force experienced by the basic N-terminal region of signal peptides upon interaction with vesicles of this composition.

Hydrophobic effect

The energy of signal peptide association with vesicles is modeled as a process of insertion of the peptide as a random coil in solution into the lipid acyl chain region in a predominantly helical structure. The maximum theoretical energy from the hydrophobic effect is estimated by calculating the net energy gained from displacement of the hydrophobic amino acids into the nonpolar lipid acyl chain region. Using the cyclohexane/water partition data of Radzicka and Wolfenden (1988), in conjunction with the residue size corrected scale of Sharp et al. (1991b), the maximum available energy from burying the hydrophobic amino acids of the LamB WT peptide is approximately 91 kcal/mol. A theoretical value of 55 kcal/mol is obtained without the Flory-Huggins correction. This large difference illustrates the magnitude of the residue size correction term for partitioning of peptides of this length. In any case, the theoretical energy from displacement of the hydrophobic residues of the signal peptides from the aqueous phase is substantial and favorable.

The actual energy gain from the hydrophobic effect can be estimated by determining the fraction of the theoretical maximum energy that is satisfied upon peptide incorporation into the bilayer. Incorporation of peptides into the anisotropic medium of lipid vesicles involves complexities that are not considered in the simple partitioning between bulk solvents. For example, the bilayer has some water content that is further modulated by peptide incorporation (companion paper). However, previous studies by Jacobs and White (1989) on a series of tripeptides of the form Ala-X-Ala-O-*tert*-butyl have shown that approximately 50–60% of the theoretical hydrophobic energy is satisfied upon binding of these peptides to the well hydrated vesicle interfacial region, without the necessity for significant penetration of the peptide backbone into the acyl chain region. This result is in agreement with well described models that state that the hydrophobic effect results from a change in bulk water structure (Tanford, 1980). Thus, although the vesicle interface is reasonably well hydrated, bulk water effects are minimal. Therefore, removal of a peptide from the aqueous phase to the vesicle interface results in a hydrophobic free energy, which is a substantial fraction of the theoretical maximum available energy from the hydrophobic effect. The signal peptides examined in the present study all show evidence of insertion into the bilayer acyl chain region (see companion paper). Therefore, because interfacial binding alone is sufficient to yield greater than 50% of the available energy, and the lipid acyl chain region is less hydrated than the interface, it is anticipated that signal peptide binding/insertion is accompanied by a large, favorable hydrophobic free energy that is a very high proportion of the theoretical maximum. The specific energy gains from the hydrophobic effect will vary somewhat among individual residues depending on their position in the bilayer, i.e., a greater energy gain is expected from well inserted residues in the core region than for residues near the termini. Nonetheless, we assume that the binding energy from the hydrophobic effect approaches that of the theoretical estimate, because the peptides are well removed from the bulk water phase.

Conformational restriction and polar interactions

The favorable interaction energy arising from electrostatic and hydrophobic effects is counterbalanced by the unfavorable energy associated with conformational restriction of the peptide and the insertion of polar side chains. Also, the unfavorable interactions of free C-termini and acidic side chains with the negatively charged vesicles contribute significantly.

The coil to helix transition, concomitant with insertion (see companion paper), involves loss of internal degrees of freedom, which has been estimated to be 1.2 kcal/mol residue (Tanford, 1962). This term represents the configurational entropy lost in restricting the peptide to an α-helix. Thus, adoption of a completely helical structure by a signal peptide would require approximately 29 kcal/mol (based on 24 peptide bonds). The cost of desolvation associated with transferring a nonbonded NH:C=O pair from water to a nonpolar solvent is estimated at approximately 6 kcal/mol (Jacobs and White 1989). This very high energetic cost associated with displacing free amide and carbonyl groups from water is the basis for the strong driving force that results in adoption of predominantly helical structure in nonpolar environments. All signal peptides examined in the present study (see companion paper) as well as other signal peptides we have analyzed (Rizo et al., 1993; Wang et al., 1993) exhibit about 70% helix in membrane-mimetic environments (companion paper). Thus, a positive free energy cost of at least 20 kcal/mol caused by configurational entropy is expected upon insertion in the bilayer acyl chain region. Also, additional positive free energy necessarily results from formation of helical structure in peptide regions in which the sequence is not conducive to formation of this structure. Nevertheless, the 6 kcal/mol associated with desolvation/insertion of free backbone groups is a strong driving force for helical structure. The actual energy loss from burying non-hydrogen-bonded backbone groups depends on the their degree of hydration in the bilayer (see below). The dynamics of secondary structure in the inserted state, therefore, are likely to be a complex function of hydration potential and intrinsic helical propensity along the length of the peptide.

In addition to the energy cost associated with secondary structure formation and insertion of free backbone groups, significant energy is required to desolvate and insert polar side chains into the bilayer interior. Theoretical energies (kcal/mol) can be estimated as follows: OH, 4; NH_2, 5.0: C=O, 2.0 kcal/mol (Jacobs and White, 1989). Thus, the net cost of burying the glutamine (position 22), serine (20), and threonine (4) residues is 15 kcal/mol, and that of burying an amidated C-terminal group is 7 kcal/mol. Also, the cost of burying the proline group is at least 2 kcal/mol because of the necessity of burying one free C=O. Analogously to

calculating the actual energy gain from the hydrophobic effect, the energetic cost of burying these side chains, as well as that for free backbone polar groups, is defined by the fractional hydration of these groups in the bilayer. The necessity to hydrate these groups at least partially almost certainly accounts for the experimental observation that increased bilayer hydration occurs upon peptide insertion as indicated by Trp fluorescence data in the companion paper. However, it is impossible to estimate meaningfully the fraction of time these groups are hydrogen-bonded without accurate estimates of bilayer water content and the strength of hydrogen bonding within the bilayer. Nevertheless, it is evident that the total energy associated with conformational restrictions and polar interactions is a significant fraction of the total gain from hydrophobic interactions.

The energy cost associated with burying negatively charged Asp residues and free carboxy termini can be modeled as arising from both specific and nonspecific effects. As discussed above, the nonspecific effect results from decreased double layer solubility, which results in an effectively lower concentration of peptide surrounding the vesicles. Specific effects result from the energy necessary to protonate the charged group and the cost of hydrating the resultant carboxylic acid group in the bilayer (Honig et al., 1986). The very unfavorable interaction of the negative charge with the negative surface probably drives protonation of negatively charged groups on the peptide. However, to analyze the energetics of this process, the hydrogen ion activity in the bilayer must be known. Estimation of this parameter is complicated by the fact that increased hydration will obviously increase bilayer proton concentration. That there is increased hydration is reflected by the low blue-shifts observed for the core aspartate mutants, as well as that observed for the WT24W peptide (see companion paper). Increased bilayer hydration necessarily involves an energy cost associated with restricting external degrees of freedom for water. However, increased hydration will also alleviate the energy cost of burying the carboxyl group. This example illustrates the difficulty in applying group additivity effects to energy calculations of this nature (Roseman, 1988).

Lipid perturbation effect

As treated by Jähnig (1983), lipid perturbation effects upon insertion of transbilayer peptides typically play an insignificant role in defining the total energetics of the system. There is a large unfavorable entropy from the lipophobic effect that arises from the ordering of the acyl chains around the peptide. However, this effect is compensated for by the favorable enthalpy associated with interaction of the hydrophobic side chains with lipid hydrophobic region. Unfortunately, the lipid perturbation effect arising from partially inserted peptides is unknown. The fact that the signal peptides show significantly stronger binding to PC-PG than PE-PG demonstrates that there exist differences in the solvation potential depending on headgroup composition. Hydration effects could be one factor: more polar interactions could be satisfied in the more hydrated PC bilayers. Alternatively, unfavorable energetics associated with cavity formation to accomodate peptide insertion could play a major role. Disruption of lipid-lipid interactions concomitant with partial peptide insertion would result in increased free volume in the core of the acyl chains leading to significant loss of packing energy. This situation may be somewhat akin to lipid monomer desorption from bilayers, an event associated with large unfavorable enthalpic changes, which receive substantial contribution from bilayer cavity formation (Nichols, 1985). Thus, it is expected that partial peptide insertion incurs significant unfavorable free energy effects.

Summary of results

Our results indicate that at approximately physiological ionic strength, hydrophobic interactions contribute significantly to the binding energy for the signal peptides. However, the apparent hydrophobic component (approximately 34 kcal/mol; taken as the difference in corrected free energy for WT-AM18W and KWK-AM) is much lower than the theoretical estimate (approximately 91 kcal/mol). Thus, the net energy gain from the hydrophobic effect is largely offset by the sum of the energy loss associated with burying polar groups, conformational restriction of the peptide, and possibly a significant lipid perturbation effect. The point mutant peptides do not show markedly different binding than that observed for WT-AM18W, although their dissociation constants are slightly higher than that for WT-AM18W, particularly for the Asp mutants. Quantitative comparison based on corrected transfer free energies is very difficult because of uncertainty in volume effects. Nonetheless, the results suggest that all the signal peptides have similar hydrophobic contributions to binding under these conditions. Thus, substitution of a single charged residue in the hydrophobic core does not reduce the energy gain from the hydrophobic effect. This result is consistent with our conclusion given in the companion paper that these peptides all insert into the lipid acyl chain region. The mutant peptides did show reduced average depths of insertion as probed by Trp fluorescence but, as discussed above, displacement of the peptides from the bulk aqueous phase into the lipid acyl chain region, regardless of insertion depth, is predicted to yield a very high fraction of the available hydrophobic binding energy.

The observation of relatively similar binding constants among the signal peptides under the high salt conditions contrasts markedly with the low salt results, where the Asp mutants show dramatically reduced lipid affinities. This result almost certainly arises from the very high energy associated with burying negatively charged groups in the bilayer interior, under these conditions. The significantly reduced affinity of the WT relative to the WT-AM peptide also supports the conclusion that a similar effect arises from burying the

free C-terminus. Thus, differences in affinity among the peptides are dominated by changes in electrostatic effects when solution ionic strength is minimal.

Taken collectively, our results indicate that the net energy associated with signal peptide-lipid interactions arises from both electrostatic and hydrophobic interactions. However, a relatively small fraction of the theoretically available hydrophobic energy (about 30%) is apparent upon binding, presumably because of losses from polar group effects. The energetics of this system are defined by a complex set of parameters, including peptide secondary structure, peptide orientation, hydration of polar groups, hydrophobic binding, and effects on lipid. Clearly, the complexity inherent in the association of these peptides with model membranes makes it impossible to distinguish quantitatively the relative contributions of each of the above factors.

The model transmembrane peptide shows much stronger binding than that observed for the signal peptides, particularly under the high ionic strength conditions, where electrostatic effects are minimized. The very high binding energy derived from the off-rate experiments strongly suggests that a much higher fraction of available hydrophobic energy is satisfied for this peptide than for the signal peptides. This result strongly supports the conclusion that unfavorable polar interactions are responsible for the relatively low binding affinities for the signal peptides. It is possible, nonetheless, that other factors discussed above may likewise contribute to differences in binding among these peptides.

Relation of results to peptide topography

The peptide topography upon interaction with lipid must correspond to the arrangement that allows maximum satisfaction of hydrophobic energy, while minimizing unfavorable polar group and lipid perturbation effects. Our results suggest that all signal peptides studied have some potential to insert into the acyl chain region of the bilayer (see companion paper). Thus, the hydrophobic driving force must be sufficient to ensure insertion, an event that may be of prime importance to the activity of these peptides in mediating protein translocation (see below). As discussed in the companion paper, the specific orientation adopted by the peptide depends on the interplay between the energetic factors discussed in this study. However, in a system of this complexity it is very difficult to define quantitatively specific energetic factors that determine signal peptide topology. Much future study with defined model peptides is necessary to address this problem.

Relation of results to other membrane-interactive peptides

These peptides behave quite differently from a number of other systems examined. For instance, the tail region of cytochrome b_5 binds to phosphatidylcholine vesicles with a significant binding constant (Leto and Holloway, 1979) as does melittin (Vogel, 1981). Signal peptides, by contrast, require a net negative charge on vesicles and thus, electrostatic interaction for significant lipid binding. This is presumably a consequence of the unique arrangement of residues in these sequences. The presence of a relatively short hydrophobic segment, punctuated by basic and polar residues, necessitates unfavorable burying of polar residues concomitant with insertion of the hydrophobic core region. This arrangement contrasts with that of transmembrane segments, which have a hydrophobic length sufficient to cross the bilayer, and with that of amphiphilic segments, which can partially insert hydrophobic residues while maintaining hydration of polar residues at the bilayer interface (for a review, see Tamm, 1991).

Relation of results to protein export

Although it is clear that various proteins are necessary for efficient translocation under most circumstances (see below), fundamental questions regarding the mechanism of this process remain unanswered. Does translocation occur via an aqueous pore composed of proteins? Or does a mechanism operate whereby protein-assisted lipid phase translocation occurs? This latter process could involve the protein moving along an interface between phospholipid and integral membrane proteins. Also, regardless of the topological details of translocation, the mechanism that maintains unidirectional protein movement across the membrane is not understood. We will consider potential insight gained from the present results regarding the thermodynamics of signal-peptide lipid interactions by addressing the following points. 1) How might membrane affinity and orientation of signal sequences affect translocation rates? 2) How might specific interactions of signal sequences with integral protein components modulate translocation?

Sec-dependent translocation is mediated by a complex array of proteins. Genetic and biochemical studies support direct interaction of the signal sequence with the peripheral membrane ATPase SecA (Puziss et al., 1989; Lill et al., 1989; Bieker-Brady and Silhavy, 1992), as well as with the integral SecE/Y complex (Bieker-Brady and Silhavy, 1992; Ito, 1984; Emr et al., 1981). Also, the integral proteins SecD and SecF, which extend a large domain into the periplasm (Schatz and Beckwith, 1990), are required for export. Sec-mediated translocation requires the energy derived from ATP hydrolysis and the protonmotive force (Δp) (Akimura et al., 1991; Brundage et al., 1992; Driessen, 1992). Recent results suggest that Δp acts during the latter stages of translocation, whereas the "translocation ATPase" activity of SecA, which requires SecY/E and acidic lipids, is necessary at the initial stage of the process (Scheibel, 1991). This result is very much in line with the putative role of the signal sequence in the initiation of translocation. Translocation then presumably proceeds via two-dimensional diffusion (Simon et al., 1992), with directionality assured by factors such as Δp (membrane potential and/or ΔpH) and likely other proteins (perhaps

SecD, F). However, it remains unclear whether Δp acts directly to translocate proteins or if it functions through the action of Sec proteins, possibly via an antiport mechanism.

Some proteins, such as M13 procoat (Wickner, 1980) and honeybee prepromelittin (Colet et al., 1989) have been shown not to require the Sec proteins for translocation, although they share the requirement for Δp. Although these proteins are smaller than most secreted proteins, Sec independence cannot arise solely on the basis of size because many other small proteins are Sec-dependent (Wickner et al., 1991). These Sec-independent proteins harbor a typical signal sequence at the N-terminus. However, they also possess an additional hydrophobic segment near the N-terminal (signal) region. It is possible that these proteins, by virtue of their enhanced hydrophobicity, are able to insert spontaneously into the lipid phase to the degree necessary to initiate translocation, after which directional movement is driven by Δp. This prediction supports the hypothesis that in Sec-dependent translocation, the Sec proteins are necessary for the initiation step, which for most proteins involves insertion of considerable polar stretches. In an intriguing study, Kuhn et al. (1987) showed that exchange of the leader regions between M13 procoat and the Sec-dependent proOmpA revealed that Sec dependence arose from the mature rather than the leader region. Thus, although the respective leader regions shared the ability to interact with the Sec machinery, the requirement for Sec-assisted translocation depended on the nature of the contiguous mature region.

The above studies demonstrate that considerable complexity exists with regard to the details of translocation under different conditions. In particular, results from the limited cases of Sec-independent translocation, in conjunction with biochemical experiments that support the involvement of SecA (and E/Y) in the early stages of translocation, suggest that membrane insertion of preproteins can occur via different mechanisms. This conclusion is further supported by genetic results from suppressor mutation experiments in which SecY (PrlA) alleles were isolated that restored translocation competence to proteins with markedly defective signal sequences (Emr et al., 1981). In effect, the requirement for a hydrophobic signal sequence was abolished (Derman et al., 1993). This example may be taken as the opposite extreme from the Sec-independent case in which additional hydrophobicity abolished the need for the Sec proteins. These results suggest that the requirement for secretion factors is highly dependent on preprotein structure and the nature of proteinaceous export factors. It is tempting to speculate that multiple (possibly convergent) pathways function to translocate secreted proteins. For example, perhaps translocation via Sec-independent and -dependent pathways operates in all cases, but for most proteins the rate of the Sec-independent pathway is negligible in comparison to the Sec-assisted process. The possibility of multiple pathways has been discussed recently by Rapoport (1991) with one involving the likely *E. coli* SRP analog ffh.

Although we must be cautious in extrapolating our biophysical results to the function of signal sequence in export, we can make certain predictions regarding potential in vivo signal sequence interactions. The net energetics of preprotein binding to membranes are most likely a complex function of protein-lipid and protein-protein interactions. Membrane phospholipid may be viewed as the reference phase for the signal sequence-mediated interaction of the preprotein with membrane-associated secretion factors. Therefore, a quantitative understanding of signal peptide-lipid interactions is the first step in determining the molecular mechanism of protein translocation. Our results suggest that, although the signal peptides examined in this study do spontaneously bind lipid (and insert into the acyl chain region; see companion paper), signal sequence partitioning into the lipid phase is not sufficient to ensure irreversible binding of the preprotein to the membrane. Rather, the high energy cost associated with inserting polar side chains (and likely some free backbone groups) results in relatively weak binding under physiological conditions. Thus, it is evident that interaction of an inserted signal sequence (and/or its contiguous mature region) with membrane protein factors that can furnish hydrogen bonding groups may dramatically modulate preprotein binding. Furthermore, specific hydrogen bonds between the preprotein and integral membrane proteins may constrain the orientation and lateral position of an inserted preprotein to a much greater degree than that which is achieved by signal sequence insertion into the lipid phase. As discussed above, an unusually high level of hydrophobicity likely provides sufficient energy for insertion of Sec-independent preproteins.

Previous results have suggested that a critical mean residue hydrophobicity is important for biological function, although this can be achieved by different combinations of hydrophobic core lengths and residue hydrophobicity (Chou and Kendall, 1990). This suggests that a hydrophobic partitioning process is critical for signal sequence function. Our earlier analysis (Hoyt and Gierasch, 1991b) showed that signal sequence function and membrane insertion is well correlated with a critical hydrophobic core mean residue hydrophobicity of 2.4 on the Kyte-Doolittle scale (Kyte and Doolittle 1982). Although the present results demonstrate inhibited peptide insertion (companion paper) of the charged mutants relative to WT, and somewhat reduced lipid affinities for the Asp mutants, little dependence of the position of a given charged residue on lipid interactions is evident within this signal sequence family. Thus, for example, the lipid interactions of the export defective A13D mutant (mean core Kyte-Doolittle hydrophobicity of 1.8) are identical to those for the export slowed G17D mutant (mean residue hydrophobicity of 2.4). However, as discussed in the companion paper, the potential for transiently deep membrane insertion may be reduced for sequences with the charge substitution in the center of the hydrophobic core as opposed to the periphery. Also, it is possible that integral proteins that function

in export have been designed evolutionarily for polar interactions with the signal sequence C-terminal region. Thus, charged (or polar; see Hoyt and Gierasch, 1991a) residues in the center of the core may be unable to interact productively with these protein factors. In any case, much future work is necessary to define completely the role of the signal sequence in export. Our results (and those in the companion paper) provide a quantitative description of the mode and energetics of the lipid interactions for this signal sequence family. Our analysis, therefore, serves as the necessary background for future biophysical studies and provides a basis for interpretation of biochemical and genetic studies of protein export.

We thank Sarah Stradley, Kim Khuan Ng, Nathan Lewis, Candace Millhouse, and Amy Ramin for technical assistance. We also thank Terry Tripplett and Dr. Josep Rizo for helpful discussions and critical reading of the manuscript.

The support of the National Institutes of Health (GM-34962 to L. M. Gierasch and postdoctoral fellowship GM13341 to J. D. Jones), the National Science Foundation (DCB-8947252 to L. M. Gierasch), and the Robert A. Welch Foundation is gratefully acknowledged.

REFERENCES

Akimura, J., S. Matsuyama, H. Tokuda, and S. Mizushima. 1991. Reconstitution of a protein translocation system containing purified SecY, SecE and SecA from *Escherichia coli*. *Proc. Natl. Acad. Sci. USA*. 88: 6545–6549.

Barany, G., and R. B. Merrifield. 1979. The Peptides. Vol. 2. E. Gross and J. Meienhofer, editors. Academic Press, New York. 1–284.

Bartlett, G. R. 1959. Phosphorus assay in column chromatography. *J. Biol. Chem.* 234:466*a*. (Abstr.)

Batenburg, A. M., R. Brasseur, J.-M. Russychaert, G. J. M. van Scharrenburg, A. J. Slotboom, R. A. Demel, and B. de Kruijff. 1988a. Characterization of the interfacial behavior and structure of the signal sequence of the *Escherichia coli* outer membrane pore protein PhoE. *J. Biol. Chem.* 263:4202–4207.

Batenburg, A. M., R. A. Demel, A. J. Verkleij, and B. de Kruijff. 1988b. Penetration of the signal sequence of the *Escherichia coli* PhoE protein into phospholipid model membranes leads to lipid specific changes in signal peptide structure and alterations of lipid structure. *Biochemistry*. 27:5678–5685.

Bieker-Brady, K., and T. J. Silhavy. 1992. Suppressor analysis suggests a multistep, cyclic mechanism for protein secretion in *Escherichia coli*. *EMBO J.* 11:3165–3174.

Briggs, M. S., L. M. Gierasch, A. Zlotnick, J. D. Lear, and W. F. DeGrado. 1985. In vivo function and membrane binding properties are correlated for *Escherichia coli* LamB signal peptides. *Science*. 228:1096–1099.

Brundage, L., C. J. Fimmel, M. Mizushima, and W. Wickner. 1992. SecY, SecE and band 1 form the membrane-embedded domain of *Escherichia coli* preprotein translocase. *J. Biol. Chem.* 267:4166–4170.

Chou, M. M., and D. A. Kendall. 1990. Polymeric sequences reveal a functional interrelationship between hydrophobicity and length of signal peptides. *J. Biol. Chem.* 265:2873–2880.

Colet, W., C. Mollay, C., G. Müller, and R. Zimmermann. 1989. Export of honeybee prepromelittin in *Escherichia coli* depends on the membrane potential but does not depend on proteins SecA and SecY. *J. Biol. Chem.* 264:10169–10176.

Derman, A. I., J. W. Puziss, P. J. Bassford, Jr., and J. Beckwith. A signal sequence is not required for protein export in prlA mutants of *Escherichia coli*. *EMBO J.* 12:879–888.

Dill, K. A. 1990. Dominant forces in protein folding. *Biochemistry*. 29: 7133–7155.

Driessen, A. J. M. 1992. Bacterial protein translocation: kinetic and thermodynamic role of atp and the protonmotive force. *TIBS*. 17:219–223.

Dryland, A., and R. C. Sheppard. 1986. Peptide synthesis. Part 8. A system for solid-phase synthesis under low pressure continuous flow conditions. *J. Chem. Soc. Perkin Trans.* 1:125–137.

Emr, S. D., S. Hanley-Way, and T. J. Silhavy. 1981. Suppressor mutations that restore export of a protein with a defective signal sequence. *Cell*. 23:79–88.

Erickson, B. W., and R. B. Merrifield. 1976. The Proteins. Vol. 2. H. Neurath and R. L. Hill, editors. Academic Press, New York. 225–527.

Flory, P. J. 1941. Thermodynamics of high polymer solutions. *J. Chem. Phys.* 9:660–671.

Honig, B. H., W. L. Hubbell, and R. F. Flewelling. 1986. Electrostatic interactions in membranes and proteins. *Annu. Rev. Biophys. Chem.* 15: 163–193.

Hoyt, D. W., and L. M. Gierasch. 1991a. A peptide corresponding to an export-defective mutant OmpA signal sequence with asparagine in the hydrophobic core is unable to insert into model membranes. *J. Biol. Chem.* 266:14406–14412.

Hoyt, D. W., and L. M. Gierasch. 1991b. Hydrophobic content and lipid interactions of wild-type and mutant OmpA signal peptides correlate with their in vivo function. *Biochemistry*. 30:10156–10163.

Huggins, M. L. 1941. Solutions of long chain compounds. *J. Chem. Phys.* 9:440–449.

Ito, K. 1984. Identification of the secY(prlA) gene product involved in protein export in *Escherichia coli*. *Mol. Gen. Genet.* 197:204–208.

Jacobs, R. E., and S. H. White. 1989. The nature of the hydrophobic binding of small peptides at the bilayer interface: implications for the insertion of transbilayer helices. *Biochemistry*. 28:3421–3437.

Jähnig, F. 1983. Thermodynamics and kinetics of protein incorporation into membranes. *Proc. Natl. Acad. Sci. USA*. 80:3691–3695.

Jain, M. K., J. Rogers, L. Simpson, and L. M. Gierasch. 1985. Effect of tryptophan derivatives on the phase properties of bilayers. *Biochim. Biophys. Acta*. 816:153–162.

Jones, J. D., C. J. McKnight, and L. M. Gierasch. 1990. Biophysical studies of signal peptides: implications for signal sequence functions and the involvement of lipid in protein export. *J. Bioenerg. Biomembr.* 22: 213–232.

Keller, R. C. A., J. A. Killian, and B. de Kruijff. 1992. Anionic phospholipids are essential for α-helix formation of the signal peptide of prePhoE upon interaction with phospholipid vesicles. *Biochemistry*. 31:1672–1677.

Killian, J. A., R. C. A. Keller, M. Struyve, A. I. P. M. de Kroon, J. Tommassen, and B. de Kruijff. 1990. Tryptophan fluorescence study of the interaction of the signal peptide of the *Escherichia coli* outer membrane protein phoe with model membranes. *Biochemistry*. 29:8131–8137.

Kim, J., M. Mosior, L. A. Chung, H. Wu, H., and S. McLaughlin. 1991. Binding of peptides with basic residues to membranes containing acidic phospholipids. *Biophys. J.* 60:135–148.

Koyanova, R., and H. J. Hinz. 1990. Metastable behavior of saturated phosphatidylethanolamines: a densitometric study. *Chem. Phys. Lipids*. 54: 67–72.

Kuhn, A., G. Kreil, and W. Wickner. 1987. Recombinant forms of M13 procoat with an OmpA leader sequence or a large carboxy-terminal extension retain their independence of SecY function. *EMBO J.* 6:501–505.

Kyte, J., and R. F. Doolittle. 1982. A simple method for displaying the hydropathic character of a protein. *J. Mol. Biol.* 157:105–132.

Leto, T. L., and P. W. Holloway. 1979. Mechanism of cytochrome b_5 binding to phosphatidylcholine vesicles. *J. Biol. Chem.* 254:5015–5020.

Leto, T. L., M. A. Roseman, and P. W. Holloway. 1980. Mechanism of exchange of cytochrome b_5 between phosphatidylcholine vesicles. *Biochemistry*. 19:1911–1916.

Lide, D. R., editor. 1990. CRC Handbook of Chemistry and Physics. CRC Press, Boca Raton, FL.

Lill, R., K. Cunningham, L. Brundage, K. Ito, D. Oliver, and W. Wickner. 1989. SecA protein hydrolyzes ATP and is an essential component of the protein translocation ATPase of *Escherichia coli*. *EMBO J.* 8:961–966.

Mayer, L. D., M. J. Hope, and P. R. Cullis. 1986. Vesicles of variable sizes produced by a rapid extrusion procedure. *Biochim. Biophys. Acta*. 858: 161–168.

McKnight, C. J., M. S. Briggs, and L. M. Gierasch. 1989. Functional and nonfunctional LamB signal sequences can be distinguished by their biophysical properties. *J. Biol. Chem.* 264:17293–17297.

McKnight, C. J., M. Rafalski, and L. M. Gierasch. 1991. Fluorescence analysis of tryptophan-containing variants of the LamB signal sequence upon insertion into a lipid bilayer. *Biochemistry*. 30:6241–6246.

McLaughlin, S. 1989. The electrostatic properties of membranes. *Annu. Rev. Biophys. Biophys. Chem.* 18:113–136.

Nichols, J. W. 1985. Thermodynamics and kinetics of phospholipid monomer-vesicle interaction. *Biochemistry*. 24:6390–6398.

Nichols, J. W., and R. E. Pagano. 1982. Use of resonance energy transfer to study the kinetics of amphiphile transfer between vesicles. *Biochemistry*. 21:1720–1726.

Pjura, W. J., A. M. Kleinfeld, and M. J. Karnovsky. 1984. Partition of fatty acids and fluorescent fatty acids into membranes. *Biochemistry*. 23:2039–2043.

Puziss, J. W., J. D. Fikes, and P. J. Bassford, Jr. 1989. Analysis of mutational alterations in the hydrophilic segment of the maltose-binding protein Signal Peptide *J. Bacteriol.* 171:2303–2311.

Radzicka, A., and R. Wolfendon. 1988. Comparing the polarities of the amino acids: side chain distribution coefficients between the vapor phase, cyclohexane, 1-octanol, and neutral aqueous solution. *Biochemistry*. 27: 1664–1670.

Rapoport, T. A. 1991. Protein translocation: a bacterium catches up. *Nature*. 349:107–108.

Rizo, J., F. J. Blanco, B. Kobe, M. D. Bruch, and L. M. Gierasch. 1993. Conformational behavior of *Escherichia coli* OmpA signal peptides in membrane mimetic environments. *Biochemistry*. 32:4881–4894.

Roseman, M. A. 1988. Hydrophilicity of polar amino acid side-chains is markedly reduced by flanking peptide bonds. *J. Mol. Biol.* 200:513–522.

Schatz, P. J., and J. Beckwith. 1990. Genetic analysis of protein export in *Escherichia coli. Annu. Rev. Genet.* 24:215–248.

Scheibel, E., A. J. M. Driessen, F-U. Hartl, and W. Wickner. 1991. Δ_{μ^+} and ATP function at different steps of the catalytic cycle of preprotein translocase. *Cell*. 64:927–939.

Schwarz, G., and G. Beschiavilli. 1989. Thermodynamic and kinetic studies on the association of melittin with a phospholipid bilayer. *Biochim. Biophys. Acta*. 979:82–90.

Sharp, K. A., A. Nicholls, R. M. Fine, and B. Honig. 1991a. Reconciling the magnitude of the microscopic and macroscopic hydrophobic effects. *Science*. 252:106–109.

Sharp, K. A., A. Nicholls, R. Friedman, and B. Honig. 1991b. Extracting hydrophobic free energies from experimental data: relationship to protein folding and theoretical models. *Biochemistry*. 30:9686–9697.

Simon, S. M., C. S. Peskin, and G. F. Oster. 1992. What drives the translocation of proteins? *Proc. Natl. Acad. Sci. USA*. 89:3770–3774.

Stader, J., S. A. Benson, and T. J. Silhavy. 1986. Kinetic analysis of *lamb* mutants suggests that the signal sequence plays multiple roles in protein export. *J. Biol. Chem.* 261:15075–15080.

Surewicz, W. K., and R. M. Epand. 1984. Role of peptide structure in lipid-peptide interactions: a fluorescence study of the binding of pentagastrin-related pentapeptides to phospholipid vesicles. *Biochemistry*. 23: 6072–6077.

Tamm, L. 1991. Membrane insertion and lateral mobility of synthetic amphiphilic signal peptides in lipid model membranes. *Biochim. Biophys. Acta*. 1071:123–148.

Tanford, C. 1962. Contribution of the hydrophobic interaction to the stability of the globular conformation of proteins. *J. Am. Chem. Soc.* 84: 4240–4247.

Tanford, C. 1980. The Hydrophobic Effect, 2nd ed. John Wiley & Sons, New York. 190.

Vogel, H. 1981. Incorporation of melittin into phosphatidylcholine bilayers. *FEBS Lett.* 134:37–42.

Wang, Z., J. D. Jones, J. Rizo, and L. M. Gierasch. 1993. Membrane-bound conformation of a signal peptide: a transferred nuclear Overhauser effect analysis. *Biochemistry*. 32:13991–13999.

Wickner, W. 1980. Assembly of proteins into membranes. *Science*. 210: 861–868.

Wickner, W., A. J. M. Driessen, and F.-U. Hartl. 1991. The enzymology of protein translocation across the *Escherichia coli* plasma membrane. *Annu. Rev. Biochem.* 60:101–124.